Thermodynamic functions as correlation-function integrals

K. Koga[1,a] and B. Widom[2]
[1]*Department of Chemistry, Faculty of Science, Okayama University, Okayama 700-8530, Japan*
[2]*Department of Chemistry, Baker Laboratory, Cornell University, Ithaca, New York 14853-1301, USA*

(Received 24 January 2013; accepted 3 March 2013; published online 21 March 2013)

Expressions of some thermodynamic functions as correlation-function integrals, such as the Ornstein-Zernike integral, the Kirkwood-Buff integrals, and the integral formulas for virial coefficients, are recalled. It is noted, as has been remarked before, that the choice of molecular centers from which intermolecular distances are measured is arbitrary and that different choices lead to different forms of the correlation functions but that the integrals must be independent of those choices. This is illustrated with the second virial coefficients of hard spheres in one, two, and three dimensions, with that of gaseous propane in three dimensions, and with computer simulations of the pair correlations in water and in a dilute aqueous solution of propane. © *2013 American Institute of Physics*. [http://dx.doi.org/10.1063/1.4795498]

I. INTRODUCTION

Thermodynamic functions or other properties of macroscopic systems may often be calculated as integrals of correlation functions. An example is the Ornstein-Zernike formula for a one-component fluid,

$$kT\chi - \frac{1}{\rho_1} = \int h_{11}(r)d\tau, \tag{1}$$

where χ is the fluid's compressibility, ρ_1 its number density, and $h_{11}(r)$ its pair correlation function as a function of the distance r between molecule centers, with k the Boltzmann constant and T the temperature. Here $d\tau$ is the element of volume in the integration, which is over the whole space.

The Kirkwood-Buff integrals[1–4] are generalizations of (1) to systems of two or more components. With two components in which component 2, the solute, is infinitely dilute in component 1, the solvent, these are, in addition to (1),

$$kT\chi - v_2 = \int h_{12}(r)d\tau, \tag{2}$$

$$B = -\frac{1}{2}\int h_{22}(r)d\tau. \tag{3}$$

In (2), χ is still the compressibility of the pure solvent while $h_{12}(r)[=h_{21}(r)]$ is the solute-solvent pair correlation function at infinite dilution and v_2 is the infinitely dilute limit of the partial molecular volume of the solute in the solvent. This is expressible in terms of χ, the pressure p, and the number densities ρ_1 and ρ_2 of the solvent and solute, by

$$v_2 = \chi\left(\frac{\partial p}{\partial \rho_2}\right)^{\circ}_{\rho_1,T}, \tag{4}$$

the superscript $^\circ$ denoting the $\rho_2 = 0$ limit. Equation (2) is also closely related to a recently discussed formula for the excess buoyant force (over that given by "Archimedes' principle") felt by large spheres, species 2, dilutely dispersed in a liquid of small molecules, species 1, in a gravitational field.[5,6] In (3), $h_{22}(r)$ is the solute-solute pair-correlation function at infinite dilution and B is the osmotic second virial coefficient. Formula (3) occurred originally in the McMillan-Mayer solution theory,[7] where it is the analog of the formula for the gas-phase second virial coefficient but with the intermolecular potential in the latter now replaced by the infinitely dilute limit of the solute-solute pair potential of mean force.

The integrands in (1)–(3) depend only on the distance r between points ("centers") arbitrarily assigned to be associated with each molecule of the pair. They are called the centers pair correlation functions by Gray and Gubbins;[8] they may be obtained by averaging the full pair correlations over the relative orientations and internal structures of the molecules of the pair, with fixed distance r between their arbitrarily defined centers.

The integrals on the right-hand sides of (1)–(3) are measures of the fluctuations in the densities of the molecular species, hence in the densities of centers, as follows from the definitions of the correlation functions $h_{ij}(r)$, while the left-hand sides measure those same fluctuations as follows from the grand canonical partition function. The left-hand sides are manifestly independent of any arbitrary choice of molecule centers, and so also must be the integrals on the right-hand sides, but their integrands $h_{ij}(r)$ do depend, often markedly, on those choices. That the molecule centers may be chosen arbitrarily while the correlation function integrals remain invariant to those choices has long been recognized.[9] That flexibility can be exploited to create pair correlation functions that simplify the subsequent integrations.[10] The assigned centers need not even lie within the molecules themselves or on any atom centers, nor need they be chosen the same on the two molecules of the pair.

Here we shall illustrate these principles in model systems, first in Sec. II with the second virial coefficient of hard spheres in 1, 2, and 3 dimensions, then in Sec. III with the second virial coefficient of gaseous propane, and in Sec. IV

[a]Electronic mail: koga@okayama-u.ac.jp.

with computer simulations of water and of propane in aqueous solution.

II. HARD SPHERES IN 1, 2, AND 3 DIMENSIONS

For hard rods of length σ confined to a line, the second virial coefficient is σ, as follows from the equation of state $p = \rho kT/(1 - \sigma\rho)$.[11] If the arbitrarily assigned "center" is chosen to be the rod center itself, as is natural, then the pair correlation function $h(|x|)$ at infinite dilution, as a function of the displacement $x = x_2 - x_1$ between the centers of the pair located at x_2 and x_1 on the line, is -1 when $|x| < \sigma$ and 0 when $|x| > \sigma$. Then the second virial coefficient B is related to the integral of that $h(|x|)$ at infinite dilution over the whole line by

$$B = -\frac{1}{2}\int_{-\infty}^{\infty} h(|x|)dx = -\int_0^{\infty} h(r)dr = \sigma, \tag{5}$$

as required.

To illustrate the remarks made in Sec. I, we now, instead, choose as the "center" of each rod a point distant b from its geometrical center. Note that when $b > \sigma/2$ this point lies outside the rod itself. As shown in Appendix A, if $b < \sigma/2$, then

$$h(r) = \begin{cases} -1, & r < \sigma - 2b \\ -3/4, & \sigma - 2b < r < \sigma \\ -1/4, & \sigma < r < \sigma + 2b \\ 0, & \sigma + 2b < r; \end{cases} \tag{6}$$

if $\sigma/2 < b < \sigma$, then

$$h(r) = \begin{cases} -1/2, & r < 2b - \sigma \\ -3/4, & 2b - \sigma < r < \sigma \\ -1/4, & \sigma < r < 2b + \sigma \\ 0, & 2b + \sigma < r; \end{cases} \tag{7}$$

and if $\sigma < b$, then

$$h(r) = \begin{cases} -1/2, & r < \sigma \\ 0, & \sigma < r < 2b - \sigma \\ -1/4, & 2b - \sigma < r < 2b + \sigma \\ 0, & 2b + \sigma < r. \end{cases} \tag{8}$$

This $h(r)$ is plotted against r/σ for $b = 0, \sigma/4, 3\sigma/4$, and $5\sigma/4$ in Fig. 1. It may be verified from (6)–(8) (or from a glance at Fig. 1) that (5) holds for all b, while $h(r)$ itself obviously depends on b. This is as we wished to see.

For hard circles of diameter σ with their centers chosen to be at their geometrical centers, one has $B = (\pi/2)\sigma^2$. If instead one chooses the center of each to lie at a distance b from the geometrical center, then, as shown in Appendix B,

$$h(r) = -\frac{1}{\pi}\int_0^{\pi} \frac{\psi(r,\theta)}{\pi} d\theta, \tag{9}$$

where

$$\psi(r,\theta) = \begin{cases} 0, & |a-b| > \sigma \\ \arccos\frac{a^2+b^2-\sigma^2}{2ab}, & |a-b| < \sigma < a+b \\ \pi, & a+b < \sigma \end{cases} \tag{10}$$

with

$$a = \sqrt{b^2 + r^2 - 2br\cos\theta}. \tag{11}$$

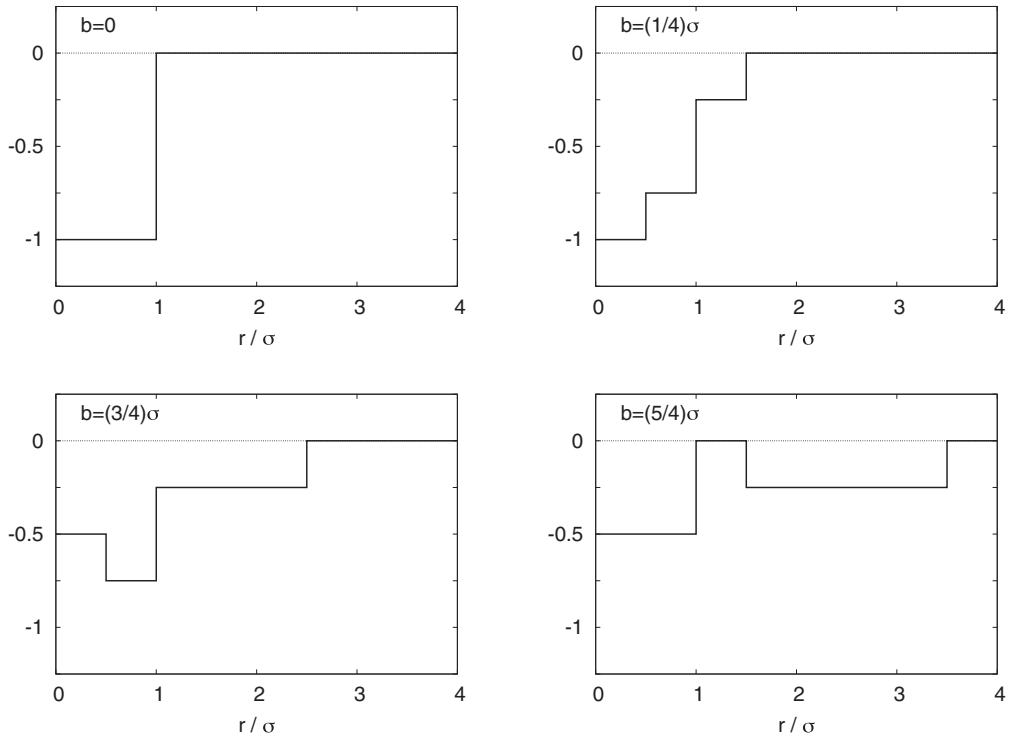

FIG. 1. The pair correlation function $h(r)$ of hard rods in the infinitely-dilute-gas limit, with four different values of b.

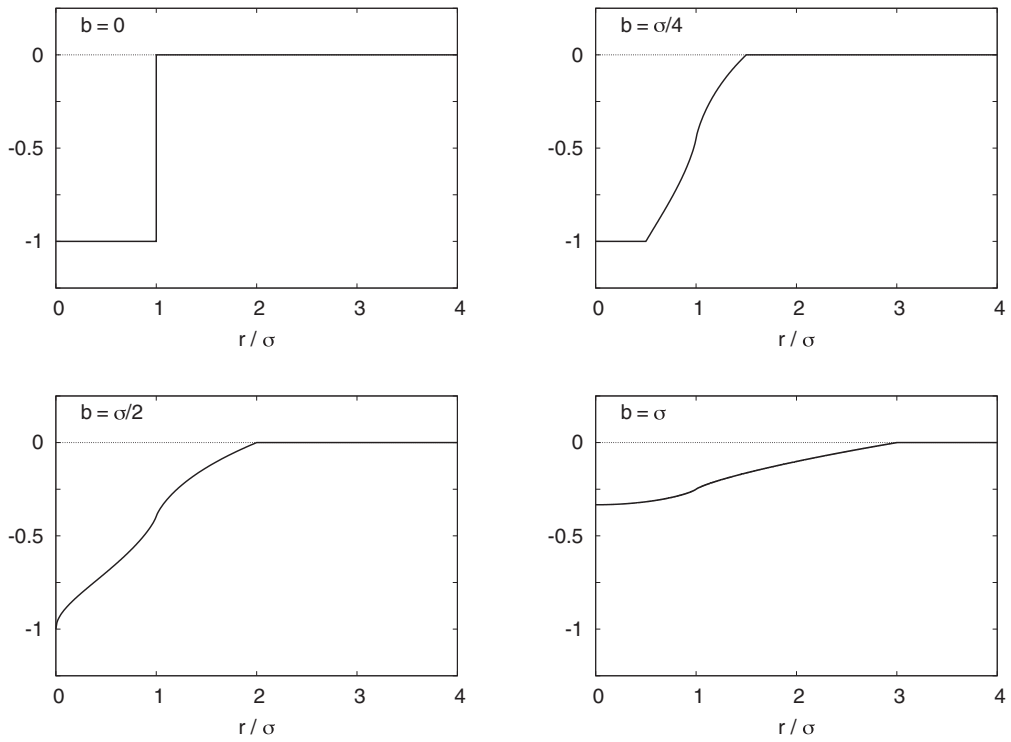

FIG. 2. The pair correlation function $h(r)$ of hard circles in the infinitely-dilute-gas limit, with four different values of b.

In Fig. 2, this $h(r)$ is plotted against r/σ for $b = 0$, $\sigma/4$, $\sigma/2$, and σ. For the last of these, the assigned center lies outside the circle. The numerically calculated integrals of $h(r)$ are $-2B = -2\pi(0.4999)\sigma^2$ for all b, as we wished to see.

For hard spheres of diameter σ, with the center chosen to be at the geometrical center of each sphere, one has $B = (2\pi/3)\sigma^3$. If instead one chooses the center of each to lie at a distance b from the geometrical center, then, as shown in Appendix C,

$$h(r) = \frac{1}{4}\int_{-1}^{1}[\cos\phi(r,\xi) - 1]d\xi, \tag{12}$$

where

$$\phi(r,\xi) = \begin{cases} 0, & |a-b| > \sigma \\ \arccos\frac{a^2+b^2-\sigma^2}{2ab}, & |a-b| < \sigma < a+b \\ \pi, & a+b < \sigma \end{cases} \tag{13}$$

with

$$a = \sqrt{b^2 + r^2 - 2br\xi}. \tag{14}$$

In Fig. 3, this $h(r)$ is plotted against r/σ for $b = 0$, $\sigma/4$, $\sigma/2$, and σ. For the last of these, the assigned center lies outside the sphere. The numerically calculated integrals of each of the $h(r)$ in Fig. 3 give $-2B = -4\pi\sigma^3$ (0.333 333), the same for all b, as we wished to see.

III. GASEOUS PROPANE

The second virial coefficient B of a gas of nonspherical molecules interacting with the pair potential $\Psi(r, \Omega_1, \Omega_2)$ is given by

$$B = -\frac{1}{2}\int[\langle e^{-\Psi(r,\Omega_1,\Omega_2)/kT}\rangle_{\Omega_1,\Omega_2} - 1]d\tau, \tag{15}$$

where r is the distance between arbitrarily assigned centers of two molecules and Ω_1, Ω_2 are the orientations of the two. The bracket $\langle\cdots\rangle_{\Omega_1,\Omega_2}$ means the unweighted, normalized average over all orientations. Here again $d\tau$ is the element of volume in the integration, which is over the whole volume. Direct evaluation of the right-hand side of (15) for given Ψ requires a multidimensional integral over the orientations and the distance, which must be done numerically,[12] except for special forms of pair potentials Ψ.[13,14] Alternatively, with the aid of simulation one may first calculate the radial distribution function $g(r)$ between arbitrarily chosen centers of molecules at low densities and then, noting that $g(r) \sim \langle e^{-\Psi(r,\Omega_1,\Omega_2)/kT}\rangle_{\Omega_1,\Omega_2}$ as $\rho \to 0$, one obtains B from the one-dimensional integral

$$B = -2\pi\lim_{\rho\to 0}\int_0^\infty [g(r) - 1]r^2 dr. \tag{16}$$

This is a special case of (3) with the "solvent" now vacuum.

To illustrate the calculation of B from $g(r)$ of a dilute gas of nonspherical molecules, we performed NVT ensemble molecular dynamics simulations of gaseous propane. The simulations here and in Sec. IV were done with GROMACS (GROningen MAchine for Chemical Simulations).[15] The simulation box is a cube of side 10 nm ($V = 1000$ nm^3), contains 20, 40, or 80 molecules, and is subject to periodic boundary conditions. The temperature is 300 K. The intermolecular interaction potential is taken to be the OPLS model, which has three Lennard-Jones (LJ) interaction sites representing two CH_3 groups and one CH_2.[16] The LJ potentials are tapered off

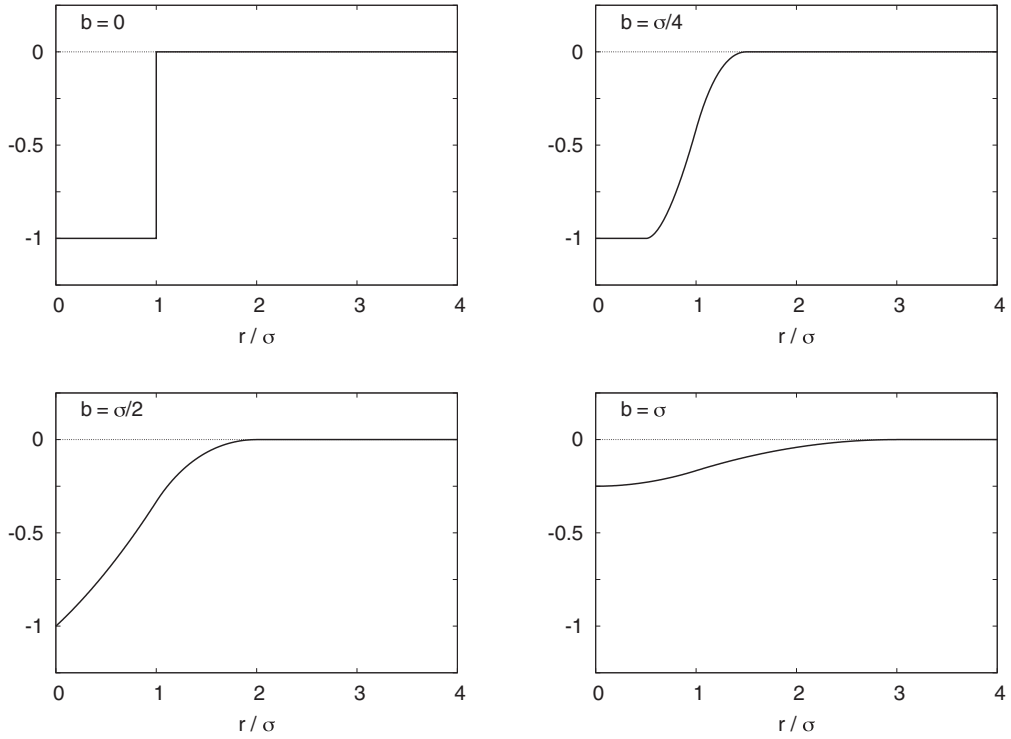

FIG. 3. The pair correlation function $h(r)$ of hard spheres in the infinitely-dilute-gas limit, with four different values of b.

by a switching function in the range 1.4 nm $< r <$ 1.7 nm. The time step is 1.0 fs. The net simulation length for production runs is 160, 1000, and 2000 ns for the system of 80, 40, and 20 molecules, respectively. The radial distribution functions are then obtained for three pairs of the interaction sites, CH_3–CH_3, CH_3–CH_2, and CH_2–CH_2, which correspond to pairs of different choices of molecule centers. The finite-size effect on $g(r)$ is not simply corrected by a factor $1 - 1/N$.[17,18] In the case of 20 molecules, $g(r) \sim 0.967$ for $r > 2.0$ nm as compared to $1 - 1/N = 0.95$. Thus each numerically obtained $g(r)$ is multiplied by a constant that makes the average value over the range 2.0 nm $< r <$ 2.5 nm equal to the correct asymptote 1. Integral (16) is then evaluated with the upper limit ∞ replaced by a finite distance R_c.

In Fig. 4 the $g(r)$ is plotted for the three choices of molecule centers of the model propane ($N = 20$, $\rho = 0.02$ nm^{-3}). All the curves have the characteristic forms of $g(r)$ for dilute gases but they are different from each other. It is confirmed that the integrals $\int_0^{R_c}[g(r) - 1]r^2dr$ converge for $R_c > 1.7$ nm. The values of the integral multiplied by -2π with $R_c = 2.4$ nm are -0.623, -0.623, and -0.622 nm^3 for the CH_3–CH_3, CH_3–CH_2, and CH_2–CH_2 pairs, respectively. They are nearly identical, as we wished to see. The invariance of the integral was also confirmed for the other densities.

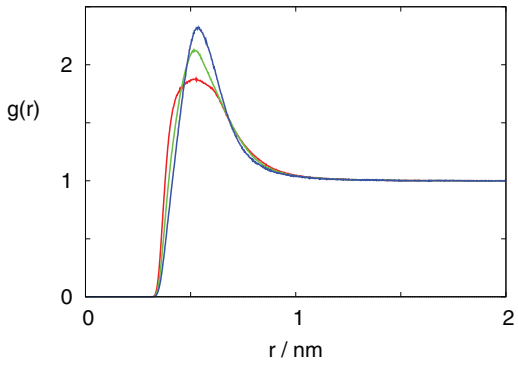

FIG. 4. The radial distribution function $g(r)$ of gaseous propane at 300 K and $\rho = 0.02$ nm^{-3} for three different pairs of the molecule "centers:" CH_3–CH_3 (first peak lowest, red), CH_3–CH_2 (middle, green), and CH_2–CH_2 (highest, blue).

The $g(r)$ at low densities may be expanded as

$$g(r) = \langle e^{-\Psi(r,\Omega_1,\Omega_2)/kT}\rangle_{\Omega_1,\Omega_2} + \rho g_1(r) + \rho^2 g_2(r) + \cdots. \tag{17}$$

Then the low-density limit of the integral (16), which is B, is obtained by linear extrapolation of the integral to $\rho = 0$. The numerically calculated integral is indeed nearly linear in ρ and the linear extrapolation gives $B = -0.60$ nm^3. It is close to -0.63 nm^3, the experimental B at 300 K,[19] although the OPLS model of propane was originally developed to fit only the liquid density and the heat of vaporization.

IV. WATER AND AN AQUEOUS SOLUTION OF PROPANE

We performed *NPT*-ensemble molecular dynamics simulations of liquid water at 298 K and 1 bar. The potential model of water is the TIP4P/2005[20] with the LJ potential truncated at 0.9 nm; the long-range Coulomb interaction is treated by the Ewald sum with the real-space cutoff of 0.9 nm. The number of molecules is 2000 and the simulation length for the production run is 2.0 ns.

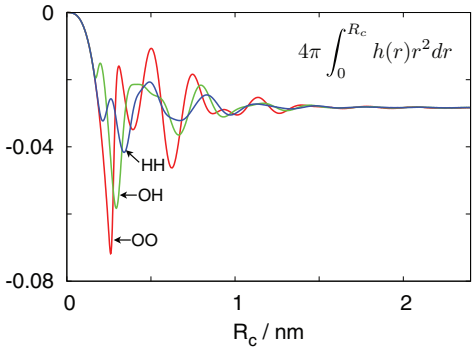

FIG. 5. The integral $4\pi \int_0^{R_c} h(r)r^2dr$, as a function of R_c in units of nm^3, of liquid water at 298 K and 1 bar for three different pairs of the molecule "centers:" O–O (red), O–H (green), and H–H (blue).

The pair correlation function $h(r)$ is obtained for O–O, O–H, and H–H interaction-site pairs, which correspond to three different choices of molecule centers. In Fig. 5, $4\pi \int_0^{R_c} h(r)r^2dr$ is plotted for the three pairs as a function of R_c. It is clearly seen that the three curves converge to a common value, as expected. With $R_c = 2.4$ nm, the value is -0.02833 ± 0.0001 nm^3, which is the right-hand side of the Ornstein-Zernike formula (1). The experimental value of $kT\chi - v$ of liquid water at 298 K and 1 bar, the left-hand side of (1), is -0.02814 nm^3. The agreement is remarkable.

We also performed *NPT*-ensemble molecular dynamics simulations of a dilute aqueous solution of propane at 298 K and 1 bar. The water-water and propane-propane intermolecular interaction potentials are the same as those for liquid water and gaseous propane employed above. The propane-water site-site potentials are the LJ potential with the parameters given by the Lorentz-Berthelot mixing rule. The LJ potential functions for the water-water, propane-water, and propane-propane intermolecular interactions are tapered off at 1.7 nm. The number of water molecules is 4000 and that of propane is 24. The simulation length for the production run is 580 ns. The propane-water and propane-propane radial distribution functions $g(r)$ are then obtained. The finite-size effect on $g(r)$ is corrected in the same way as was done for $g(r)$ of gaseous propane.

In Fig. 6 are plotted the propane-water $g(r)$ and the corresponding integral for four different pairs of the interaction sites, CH_3–O, CH_3–H, CH_2–O, and CH_2–H. That the integrals converge to a common value as shown in Fig. 6(b) illustrates that the left-hand side of (2) is independent of the choice of molecule centers. An average value of the integrals with $R_c = 2.0$ nm is -0.110 nm^3, which is very close to -0.116 nm^3, an experimental value of $kT\chi - v_2$ with $v_2 = 0.117$ nm^3.[21]

In Fig. 7 shown are the propane-propane radial distribution function $g(r)$ and the corresponding integral for three different pairs of the interaction sites, CH_3–CH_3, CH_3–CH_2, and CH_2–CH_2. The result shown in Fig. 7(b) illustrates again that the correlation function integral is invariant to the choice of molecule centers. If one assumes the concentration of propane in water is sufficiently low, then, from the McMillan-Mayer formula (3), the integral multiplied by $-1/2$ would be a good estimate of B, the osmotic second virial coefficient of propane in water. With the average value of the integrals with $R_c = 2.0$ nm, one finds $B = -0.068$ nm^3 $= -40.9$ cm^{3}mol^{-1}. The negative sign indicates an effective attraction between propane molecules in water, but the absolute value is very small as compared with the value -570 cm^{3}mol^{-1} evaluated from the van der Waals two-component equation of state[22,23] or the -668 cm^3/mol[24] as calculated with the UNIQUAC equation of state.[25] The calculated osmotic virial coefficient B is even less negative than B for gaseous propane at the same temperature.

While Fig. 7(b) illustrates the invariance of the correlation-function integral to the choice of molecular centers, which was our main point, the numerical discrepancy between the osmotic virial coefficient found in the simulations and that obtained by thermodynamics from equations of state remains an unresolved puzzle. A possible explanation is that the simulated solution, while very dilute, may still have been too concentrated for the calculated propane-propane $g(r)$ to have been effectively at infinite dilution, as required for (3) to hold. We note that the propane mole fraction in the model system was 0.006, about two hundred times the experimental equilibrium solubility, 0.27×10^{-4}, at 298 K and 1 bar.[26] That means the simulated solution may have been in a metastable rather than stable thermodynamic state. That

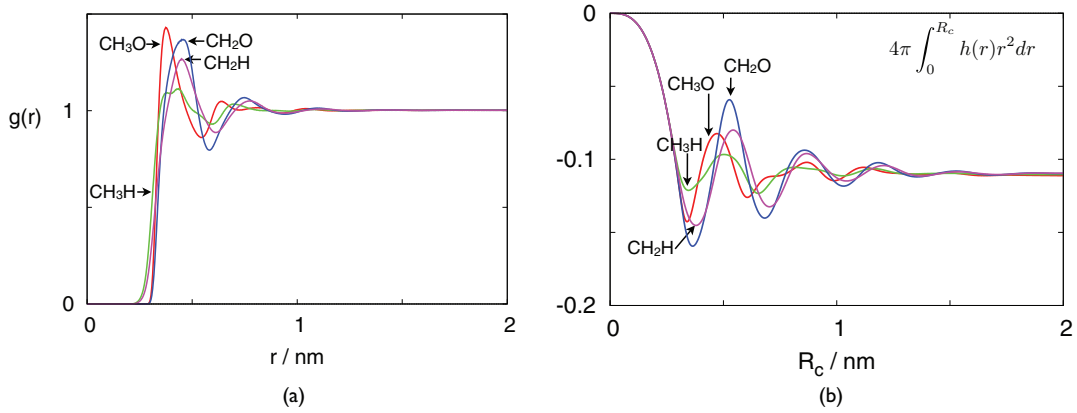

FIG. 6. (a) The propane-water $g(r)$ and (b) the corresponding integral $4\pi \int_0^{R_c} h(r)r^2dr$, as a function of R_c in units of nm^3, for a dilute aqueous solution of propane at 298 K and 1 bar. Four curves in each plot are those evaluated for pairs of the molecule "centers:" CH_3–O (red), CH_3–H (green), CH_2–O (blue), and CH_2–H (pink).

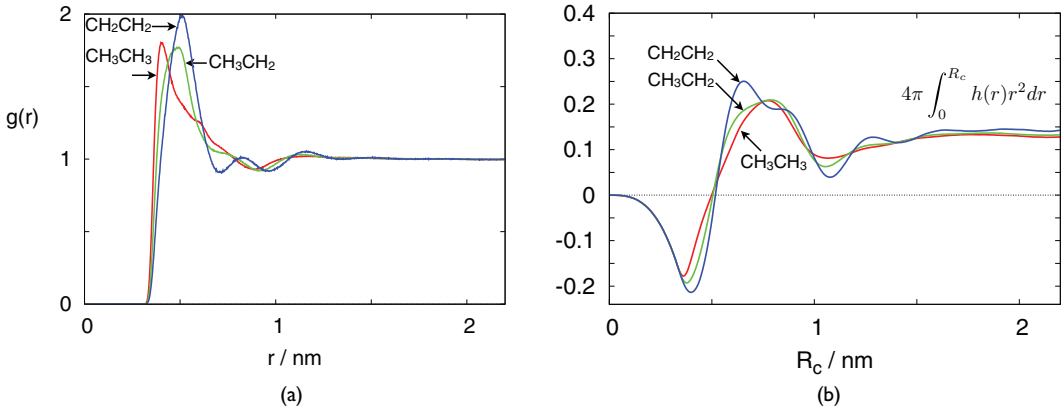

FIG. 7. (a) The propane-propane $g(r)$ and (b) the corresponding integral $4\pi \int_0^{R_c} h(r)r^2 dr$, as a function of R_c in units of nm^3, for a dilute aqueous solution of propane at 298 K and 1 bar. Three curves in each plot are those evaluated for pairs of the molecule "centers:" CH_3–CH_3 (red), CH_3–CH_2 (green), and CH_2–CH_2 (blue).

in itself would not have invalidated the calculated B,[23] but it was observed in the thermodynamic calculation that the derived B becomes rapidly unreliable for mole fractions of propane greater than about 3×10^{-4}, because higher order terms in the virial expansion may then begin to be important, or because of an incipient instability of the solution, or both.[23] This criterion for reliability of the calculation from an equation of state need not be the same as for the calculation as a correlation-function integral, but it may be. There remains also the uncertainty about the adequacy of the TIP4P model for water and OPLS for propane in this application, although we saw that in other respects they have performed well. Finally, the equations of state used in the thermodynamic calculations may have been inadequate for B, although the parameters in them were fit to reproduce other of the experimental properties of water and of aqueous solutions of propane. Clearly, more needs to be done to resolve this discrepancy.

V. SUMMARY

Some thermodynamic functions may be identified with integrals of pair correlation functions. Examples are the Ornstein-Zernike relation (1), the Kirkwood-Buff relation (2) for a solute 2 at infinite dilution in a solvent 1, and the McMillan-Mayer relation (3) for the second osmotic virial coefficient B of a dilute solute 2 in solution. The same (3) with $h_{22}(r)$ in the absence of solvent is also the formula for the second virial coefficient of species 2 in the gas phase. The pair correlation functions $h_{ij}(r)$ are functions only of the distance r between arbitrarily assigned "centers" of the two molecules of the pair. These functions depend, in general, on that assignment but their integrals, which are thermodynamic functions, do not. This fact is illustrated in several model systems: for the integral of the pair correlation function of hard spheres in 1, 2, and 3 dimensions (Sec. II), for the integral of the pair correlation function of gaseous propane as determined by NVT molecular dynamics simulations (Sec. III), and for the integrals of the water-water, propane-water, and propane-propane pair correlation functions in dilute aqueous solutions of propane as determined by NPT molecular dynamics simulations (Sec. IV). The integral of the gaseous propane-propane pair correlation function determined in the simulations yields a second virial coefficient in good agreement with experiment. The integral of the simulated pair correlation function in liquid water yields $kT\chi - v$ also in good agreement with experiment, as does the integral of the propane-water pair correlation function. The integral of the propane-propane pair correlation function as determined in the simulations of the model dilute aqueous solution of propane, while invariant to the choice of molecular centers, yields a propane-propane second osmotic virial coefficient different from that found in earlier calculations from equations of state. Possible reasons for the discrepancy are discussed but it remains unresolved.

ACKNOWLEDGMENTS

We thank Dr. Robin C. Underwood for instruction in the use of GROMACS and Dr. Noriko Yamamoto for implementing the molecular dynamics simulations of an aqueous solution of propane. The work of K.K. was supported by a Grant-in-Aid for Scientific Research from MEXT, Japan. The work of B.W. was supported by the National Science Foundation Grant No. CHE-0842022.

APPENDIX A: HARD RODS WITH ARBITRARILY CHOSEN CENTERS

Here we derive (6)–(8) for the correlation functions $h(r)$ of hard rods with arbitrarily chosen "centers" in the low-density limit. Consider two hard rods of length σ confined to a line as shown in Fig. 8. Their "centers" A and B are distant $b(>0)$ from their geometrical centers C_1 and C_2, respectively. Let x be the position of B measured from A and let θ_1 and θ_2 be the angles of $\overrightarrow{AC_1}$ and $\overrightarrow{BC_2}$, respectively, which represent the orientations of the two rods. In the case of Fig. 8, $\theta_1 = 0$ and $\theta_2 = \pi$. The orientation-dependent pair correlation function at infinite dilution is

$$h(x, \theta_1, \theta_2) = \mathrm{e}^{-\Psi(x,\theta_1,\theta_2)/kT} - 1, \tag{A1}$$

where $\Psi(x, \theta_1, \theta_2)$ is the pair potential between hard rods: $\Psi = 0$ if the two rods do not overlap and $\Psi = \infty$ if they do. There are four possible sets of orientations: $(\theta_1, \theta_2) = (0, 0)$,

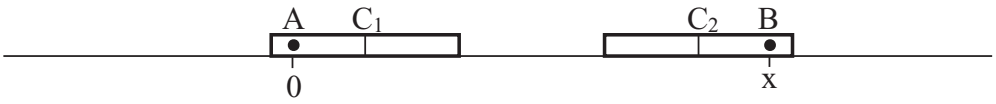

FIG. 8. Two hard rods with the geometrical centers C_1 and C_2 and the arbitrarily chosen "centers" A and B.

(π, π), $(0, \pi)$, and $(\pi, 0)$. For $(0, 0)$ and (π, π),

$$h(x, \theta_1, \theta_2) = \begin{cases} -1, & -\sigma < x < \sigma \\ 0, & \text{otherwise;} \end{cases} \tag{A2}$$

for $(0, \pi)$,

$$h(x, \theta_1, \theta_2) = \begin{cases} -1, & -\sigma + 2b < x < \sigma + 2b \\ 0, & \text{otherwise;} \end{cases} \tag{A3}$$

and for $(\pi, 0)$,

$$h(x, \theta_1, \theta_2) = \begin{cases} -1, & -\sigma - 2b < x < \sigma - 2b \\ 0, & \text{otherwise.} \end{cases} \tag{A4}$$

Note that in each case the range of x where $h(x, \theta_1, \theta_2) = -1$ is 2σ, as it should be. The pair correlation function $h(x)$ is the unweighted average of $h(x, \theta_1, \theta_2)$ over the four possible sets of orientations; the resulting $h(x)$ depends on b but by symmetry it is always even in x, i.e., $h(r)$ with $r = |x|$. For $0 < b < \sigma/2$, $\sigma/2 < b < \sigma$, and $\sigma < b$, one finds the three classes of $h(r)$ given by Eqs. (6)–(8) and illustrated in Figs. 1(b)–1(d).

APPENDIX B: HARD CIRCLES WITH ARBITRARILY CHOSEN CENTERS

In this appendix we show that in the low-density limit the pair correlation function $h(r)$ of hard circles of diameter σ with arbitrarily chosen "centers" distant b from their geometrical centers is given by (9)–(11). Figure 9 shows two hard circles 1 and 2 with geometrical centers C_1 and C_2 and chosen centers A and B, respectively. Let $\theta = \angle BAC_1$ and $\psi' = \angle C_1BC_2$. (In the figure the latter angle is denoted by ψ, which is a special angle formed by the two hard circles touching.) Then, with A and B fixed and a distance r apart in the plane, $h(r)$ is an unweighted average of

$$h(r, \theta, \psi') = e^{-\Psi(r,\theta,\psi')/kT} - 1 \tag{B1}$$

over θ and ψ', which is obtained as follows. First we calculate

$$h(r, \theta) = \langle h(r, \theta, \psi') \rangle_{\psi'},$$

an unweighted average of (B.1) over ψ', the orientation of circle 2. When ψ' varies while the points A, B, and C_1 are fixed, and so r and θ are fixed, the point C_2 moves on a circle with center B and radius b (call it circle B). If C_2 is inside the circle with center C_1 and radius σ (the dashed circle as shown in Fig. 9), the two hard circles overlap and so $h(r, \theta, \psi') = -1$; otherwise $h(r, \theta, \psi') = 0$. Therefore, $h(r, \theta)$ is the negative of the fraction of the circumference of circle B that lies inside the dashed circle: denoting that fraction by $\psi(r, \theta)/\pi$,

$$h(r, \theta) = -\frac{\psi(r, \theta)}{\pi}. \tag{B2}$$

The $h(r)$ is then an unweighted average of $h(r, \theta)$ over θ, i.e.,

$$h(r) = -\frac{1}{\pi} \int_0^\pi \frac{\psi(r, \theta)}{\pi} d\theta, \tag{B3}$$

which is (9). Let $a = BC_1$, which is given by (11). Then, if $a + b < \sigma$, circle B is entirely inside the dashed circle and so $\psi/\pi = 1$; if $|a - b| > \sigma$, circle B is entirely outside the dashed circle and so $\psi/\pi = 0$; and if $a + b > \sigma$ and $|a - b| < \sigma$, circle B is partially inside the dashed circle and so $0 < \psi/\pi < 1$. In the last case ψ is identical to the angle ψ as shown in Fig. 9 that satisfies

$$\sigma^2 = a^2 + b^2 - 2ab \cos \psi. \tag{B4}$$

This is the second equality of (10). We note that the ψ of (10) as a function of a and b is continuous at $|a - b| = \sigma$ and $a + b = \sigma$ in the a, b plane, except when $a = \sigma$ and $b = 0$ or when $a = 0$ and $b = \sigma$.

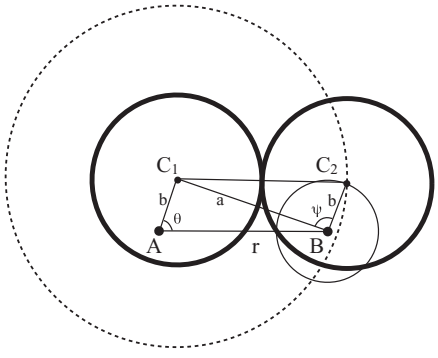

FIG. 9. Two contacting hard circles with the geometrical centers C_1 and C_2 and the arbitrarily chosen "centers" A and B. The dashed circle is the excluded circle. The small circle with center B and radius b is the one on which C_2 moves when the orientation of circle 2 varies while the chosen "center" B is fixed.

APPENDIX C: HARD SPHERES WITH ARBITRARILY CHOSEN CENTERS

Here we show that in the low-density limit the pair correlation function $h(r)$ of hard spheres with arbitrarily chosen centers is given by (12)–(14). Consider two hard spheres 1 and 2 with the geometrical centers C_1 and C_2 and the chosen "centers" A and B, respectively, with the following distances: $r = AB$ and $b = AC_1 = BC_2$. The orientation-dependent correlation function is

$$h(r, \Omega_1, \Omega_2) = e^{-\Psi(r,\Omega_1,\Omega_2)/kT} - 1, \tag{C1}$$

where Ω_1 and Ω_2 denote orientations of spheres 1 and 2 and Ψ is the hard sphere potential. First we fix A, B, and C_1 in space. Figure 10 shows the plane on which A, B, and C_1 are fixed and the cross section of sphere 1 (thick circle). When

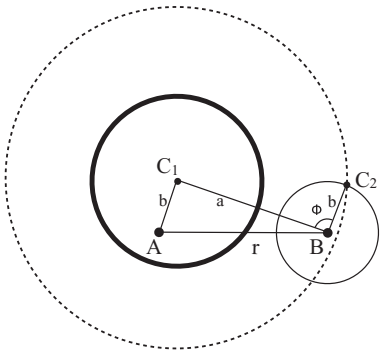

FIG. 10. A hard sphere (thick line) with diameter σ and "center" A chosen to be distance b from the geometrical center C_1, the excluded sphere (dashed line) with radius σ, and sphere B (thin line) with center B and radius b. Shown here are the plane C_1AB and the cross sections of the spheres.

the orientation of sphere 2 varies with B fixed, the geometrical center C_2 moves on a sphere with center B and radius b (we call it sphere B). If C_2 is inside a sphere with center C_1 and radius σ (we call it the excluded sphere), then $h(r, \Omega_1, \Omega_2) = -1$; otherwise $h(r, \Omega_1, \Omega_2) = 0$. Therefore, $h(r, \Omega_1)$ is the negative of the fraction of the surface of sphere B that lies inside the excluded sphere: denoting that fraction by $(1 - \cos\phi)/2$,

$$h(r, \Omega_1) = \frac{\cos\phi - 1}{2}. \tag{C2}$$

Let $a = \mathrm{BC}_1 = \sqrt{b^2 + r^2 - 2br\xi}$ with ξ the cosine of $\angle \mathrm{BAC}_1$. If $|a - b| > \sigma$, sphere B is entirely outside the excluded sphere so $\phi = 0$; if $a + b < \sigma$, sphere B is entirely inside the excluded sphere and so $\phi = \pi$; and if $|a - b| < \sigma$ and $a + b > \sigma$, then the surface of sphere B is partially inside the excluded sphere and that fraction is $(1 - \cos\phi)/2$ with ϕ defined as $\angle \mathrm{C}_1\mathrm{BC}_2$ in the geometry that C_2 lies on the intersection of sphere B and the excluded sphere, as illustrated in Fig. 10: that ϕ is given by

$$\phi = \arccos\frac{a^2 + b^2 - \sigma^2}{2ab}. \tag{C3}$$

The unweighted average of $h(r, \Omega_1)$ over Ω_1 is

$$h(r) = \frac{1}{4\pi}\int \frac{\cos\phi - 1}{2} d\Omega_1 = \frac{1}{4}\int_{-1}^{1} [\cos\phi(r, \xi) - 1] d\xi, \tag{C4}$$

which is Eq. (12).

[1] J. G. Kirkwood and F. P. Buff, J. Chem. Phys. **19**, 774 (1951).
[2] B. H. Zimm, J. Chem. Phys. **21**, 934 (1953).
[3] A. Ben-Naim, *Water and Aqueous Solutions: Introduction to a Molecular Theory* (Plenum, 1974), p. 142.
[4] A. Ben-Naim, J. Chem. Phys. **67**, 4884 (1977).
[5] R. Piazza, S. Buzzaccaro, E. Secchi, and A. Parola, Soft Matter **8**, 7112 (2012).
[6] M. Wilson, Phys. Today **65**, 15 (2012).
[7] W. G. McMillan and J. E. Mayer, J. Chem. Phys. **13**, 276 (1945).
[8] C. G. Gray and K. E. Gubbins, *Theory of Molecular Fluids, Volume 1: Fundamentals* (Clarendon Press, 1984), p. 162.
[9] J.-P. Hansen and I. R. McDonald, *Theory of Simple Liquids*, 2nd ed. (Academic Press, 1986), pp. 442, 447.
[10] D. M. Lockwood and P. J. Rossky, J. Phys. Chem. B **103**, 1982 (1999).
[11] See, for example, A. Ben-Naim, *Statistical Thermodynamics for Chemists and Biochemists* (Plenum Press, 1992), p. 230; B. Widom, *Statistical Mechanics* (Cambridge University Press, 2002) p. 109.
[12] C. Menduiña, C. McBride, and C. Vega, Phys. Chem. Chem. Phys. **3**, 1289 (2001).
[13] A. Isihara, J. Chem. Phys. **18**, 1446 (1950).
[14] T. Kihara, Adv. Chem. Phys. **5**, 147 (1963).
[15] B. Hess, C. Kutzner, D. van der Spoel, and E. Lindahl, J. Chem. Theory Comput. **4**, 435 (2008).
[16] W. L. Jorgensen, J. D. Madura, and C. J. Swenson, J. Am. Chem. Soc. **106**, 6638 (1984).
[17] J. L. Lebowitz and J. K. Percus, Phys. Rev. **122**, 1675 (1961).
[18] A. Perera, L. Zoranić, F. Sokolić, and R. Mazighi, J. Mol. Liq. **159**, 52 (2011).
[19] *Handbook of Chemistry and Physics*, 90th ed., edited by D. R. Lide (CRC, 2009), p. 6-43.
[20] J. L. F. Abascal and C. Vega, J. Chem. Phys. **123**, 234505 (2005).
[21] J. C. Moore, R. Battino, T. R. Rettich, Y. P. Handa, and E. Wilhelm, J. Chem. Eng. Data **27**, 22 (1982).
[22] B. Widom and R. C. Underwood, J. Phys. Chem. B **116**, 9492 (2012).
[23] B. Widom and K. Koga, J. Phys. Chem. B **117**, 1151 (2013).
[24] H. Liu and E. Ruckenstein, J. Phys. Chem. B **102**, 1005 (1998).
[25] J. M. Prausnitz, R. N. Lichtenthaler, and E. Gomes de Azevedo, *Molecular Thermodynamics of Fluid Phase Equilibria*, 2nd ed. (Prentice-Hall, 1986), pp. 238–245.
[26] W. Wilhelm, R. Battino, and R. J. Wilcock, Chem. Rev. **77**, 219 (1977).